

ADVANCED PLASMA SOURCES FOR SPACE APPLICATIONS

Paola De Carlo

CISAS - Università degli studi di Padova
Corso di dottorato in Scienze Tecnologie e Misure Spaziali
Curriculum: STASA

October 20th, 2017

Outline

- 1 Framework
- 2 Motivation, and objectives
- 3 Numerical Tools
- 4 Physical Assessment
- 5 Plasma Antenna Design
- 6 Source Realization, and Testing
- 7 Conclusions

Framework

Plasma exhibits complex Electromagnetic (EM) wave phenomena.
It can be exploited in a broad range of advanced application:

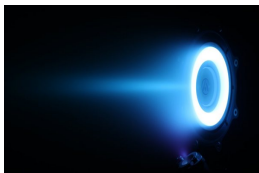
Framework

Plasma exhibits complex Electromagnetic (EM) wave phenomena.
It can be exploited in a broad range of advanced application:



Space Propulsion:

Plasma Thrusters



Space Communication:

Gaseous Plasma Antennas



Framework

Plasma propulsion systems

Use electric power to ionize the propellant and impart kinetic energy to the plasma.

Critical issues:

- Limited lifetime
- Need for an external cathode
- Low power density.

Framework

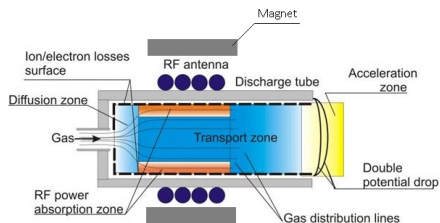
Plasma propulsion systems

Use electric power to ionize the propellant and impart kinetic energy to the plasma.

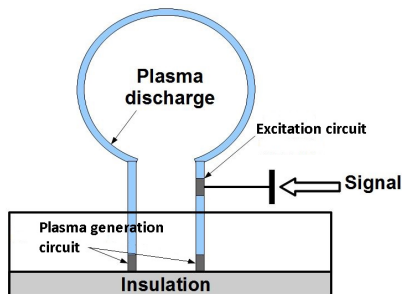
Critical issues:

- Limited lifetime
- Need for an external cathode
- Low power density.

Helicon Plasma Thruster (HPT)



Framework



Gaseous Plasma Antennas (GPAs)

Devices relying on an ionized gas to radiate EM waves.

Features:

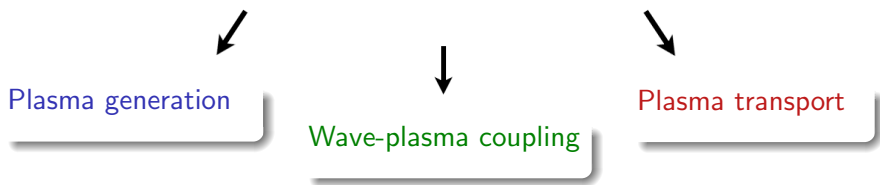
- Electrically reconfigurable;
- Low RCS, and thermal noise;
- Minimize co-site interference and signal degradation;
- Virtually *transparent* above the plasma frequency and *invisible* once turned off.

Motivation, and Objectives

Although different in shape, fields of applications, and working conditions,
GPAs and HPTs share:

Motivation, and Objectives

Although different in shape, fields of applications, and working conditions, GPAs and HPTs share:



Motivation, and Objectives

Objectives

- Physical investigation into plasma generation, charged particle transport in a magnetized plasma, and wave-plasma coupling mechanism
- Clarify the role of the antenna in the source of HPTs, and the behavior of GPAs taking into account realistic excitation circuit and plasma transport
- Coupling of the EM solution with the plasma transport
- Design, and development of innovative plasma sources to be exploited as a GPA.

Global Model

Plasma transport within a plasma source modeled by a 0-D fluid model.

Input

- Source Geometry: R , L ;
- Neutral pressure p_n ;
- Deposited power P ;

Output

- Average plasma density $n_e = n_i$;
- Average electron temperature T_e .

From input to output

System at equilibrium:

- Particles produced chemically = Particles lost in walls
- EM deposited power = Chemical losses + wall losses

ADAMANT

Wave-plasma coupling modeled by an **EM solver**.

- Full-wave approach
- Coupled surface and volume integral equations
- Arbitrarily-shaped circuit
- Inhomogeneous and anisotropic plasma

Plasma Model

- cold, and collisional
- multispecies
- non-uniform
- if magnetized, $B_0 \parallel z$ axis



ADAMANT

Wave-plasma coupling modeled by an EM solver.

- Full-wave approach
- Coupled surface and volume integral equations
- Arbitrarily-shaped circuit
- Inhomogeneous and anisotropic plasma

Plasma Model

- cold, and collisional
- multispecies
- non-uniform
- if magnetized, $B_0 \parallel z$ axis

Dyadic Permittivity Function

$$\bar{\epsilon}_{rk} = \begin{bmatrix} S_k & jD_k & 0 \\ -jD_k & S_k & 0 \\ 0 & 0 & P_k \end{bmatrix}$$

ADAMANT

Input

- Plasma mesh;
- PEC mesh;
- Source type, number of feeding points, f ;
- Gas Type;
- n_e , n_i , T_e , T_i , B_0 , p_n .

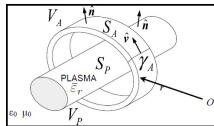
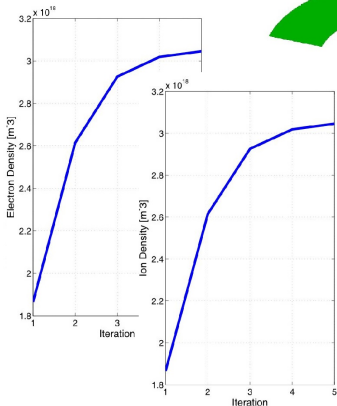
Output

- Current distributions;
- Z-matrix, S-parameters;
- Scattered fields;
- Input, absorbed, and radiated power.

From input to output

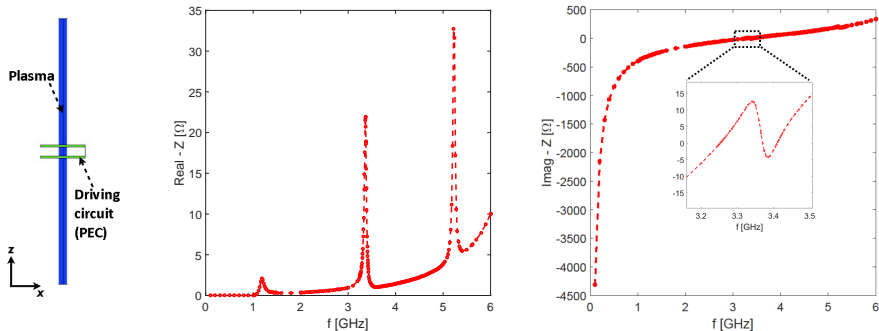
- Surface Integral Equation
- Volume Integral Equation
- Excitation on the feeding port (voltage-gap approximation)

Global Model and ADAMANT coupling



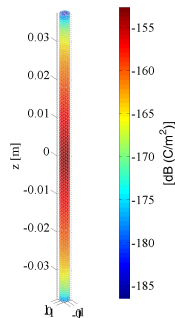
Absorbed Power

Antenna Input Impedance, and Current Distribution

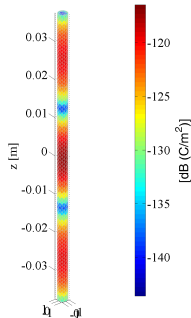


Cylindrical argon plasma column with: $n_0 = 1 \cdot 10^{19} \text{ m}^{-3}$, $T_e = 3 \text{ eV}$,
 $p_n = 0.02 \text{ mbar}$, $L = 75 \text{ mm}$, and $\Phi = 2.5 \text{ mm}$

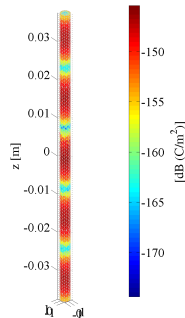
Antenna Input Impedance, and Current Distribution



$f = 1.37$ GHz



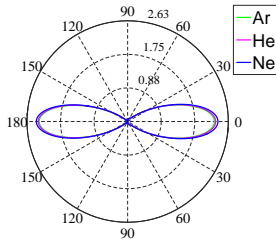
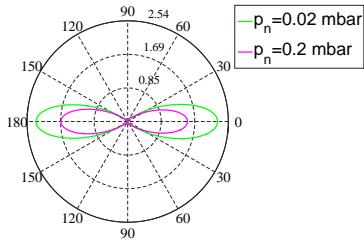
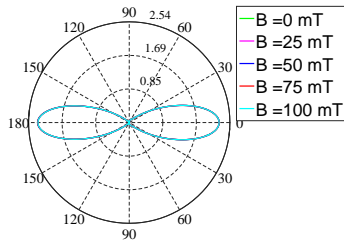
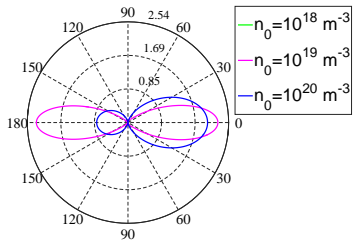
$f = 3.62$ GHz



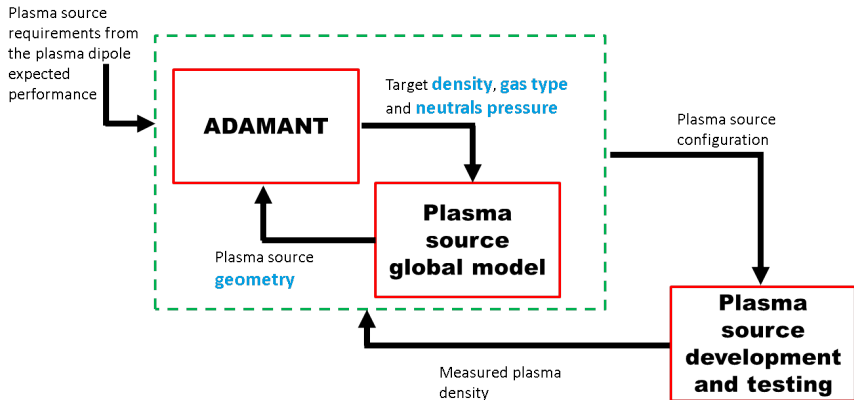
$f = 5.51$ GHz

Cylindrical argon plasma column with: $n_0 = 1 \cdot 10^{19} \text{ m}^{-3}$, $T_e = 3 \text{ eV}$,
 $p_n = 0.02 \text{ mbar}$, $L = 75 \text{ mm}$, and $\Phi = 2.5 \text{ mm}$

The GPA Radiation Pattern



Numerical, and Experimental Approach



Numerical Analysis - Plasma Source

Matlab genetic algorithm + Global Model

| Decision-space variable | Optimization parameters |
|---------------------------------|--|
| Plasma Radius Plasma Length | Plasma density of 10^{19} m^{-3} |
| Neutral Pressure Input Power | Minimize input power |

| | |
|--------------------------|------------|
| Plasma Radius [mm] | 5 - 10 |
| Plasma Length [mm] | 50 - 75 |
| Neutral Pressure [mbar] | 0.06 - 0.5 |
| Input Power [W] | 20 - 100 |

Numerical Analysis - Plasma Source

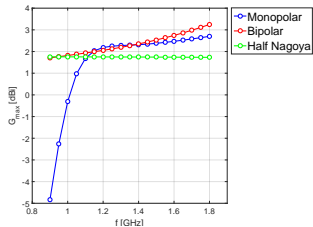
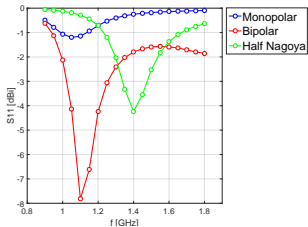
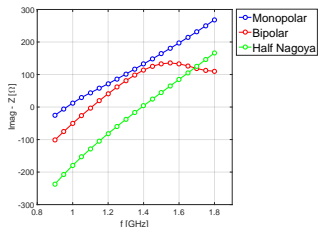
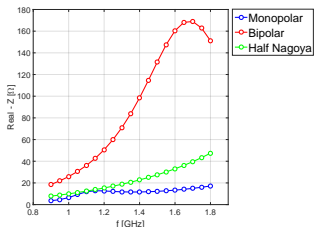
Matlab genetic algorithm + Global Model

| | Case 1 | Case 2 | Case 3 | Case 4 |
|--------------------------|---------------|---------------|---------------|---------------|
| Plasma Radius [mm] | 8.7 | 6.6 | 7.5 | 6.42 |
| Plasma Length [mm] | 54.6 | 56.2 | 78.9 | 72.5 |
| Neutral Pressure [mbar] | 0.75 | 0.39 | 0.09 | 0.4 |
| Input Power [W] | 84.1 | 23.8 | 94.2 | 28.9 |

Numerical Analysis - Antenna Performances

| | |
|--|------------------------------------|
| Coupler | Sleeve, Half-Nagoya |
| Metal-coupler length | 30 – 42 mm |
| Metal-coupler Φ | 14 – 30 mm |
| Antenna Configurations | Monopolar, Bipolar |
| Plasma Φ | 3 – 10 mm |
| Column length | 50 – 130 mm |
| Column distance | 0 – 12 mm |
| Neutral gas | Ar, He, Ne |
| Electron temperature | 3 eV |
| Neutral pressure | 0.5 – 10 mbar |
| Plasma density | $10^{18} - 10^{19} \text{ m}^{-3}$ |
| Working frequency | 0.8 – 1.8 GHz |
| Voltage | 1 V |

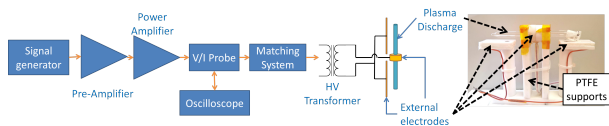
Numerical Analysis - Antenna Performances



Generation Method

Plasma generation: 2 techniques

RF - External Electrodes



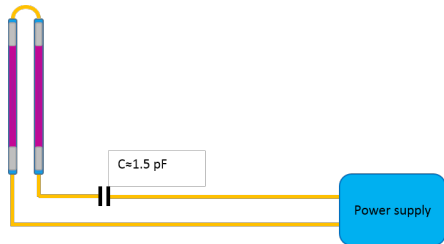
$$p_n = 1 - 10 \text{ mbar}$$

$$\phi = 3 - 10 \text{ mm}$$

Not-uniform n_e

$$n_e < 1 \cdot 10^{19} \text{ m}^{-3}$$

HF - Internal Electrodes



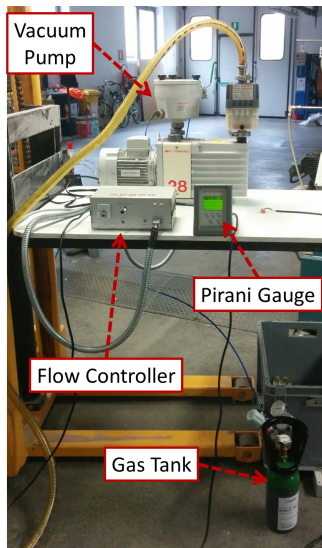
$$p_n = 1 - 2 \text{ mbar}$$

$$\phi = 5 - 6 \text{ mm}$$

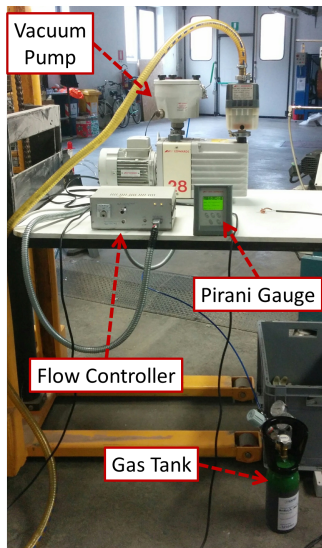
Higher, and more uniform n_e

Dirty atmosphere

Manufacturing



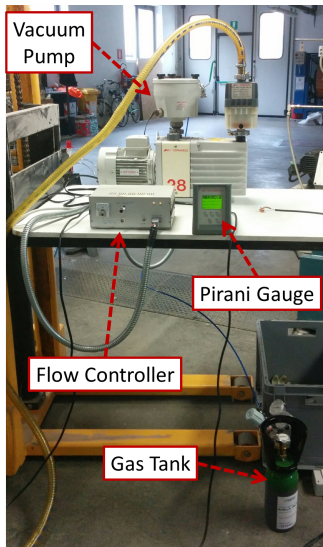
Manufacturing



Pyrex vessel with *ad hoc* interface



Manufacturing

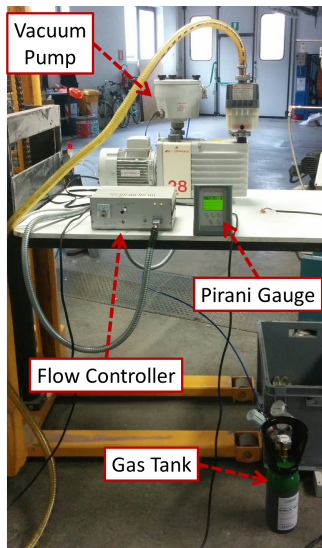


Pyrex vessel with *ad hoc* interface

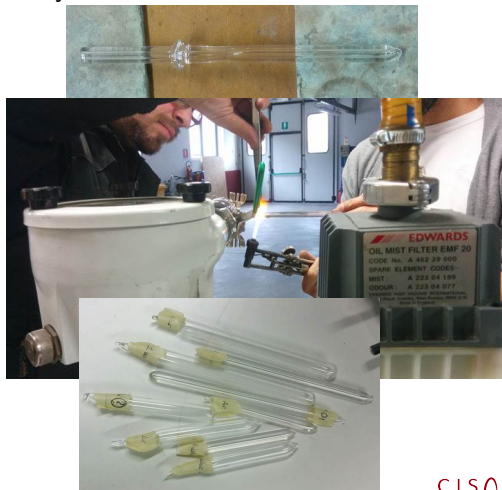


Sealing process

Manufacturing



Pyrex vessel with *ad hoc* interface

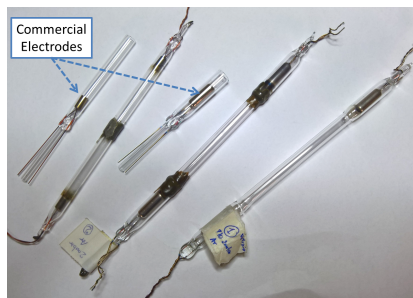


Closed vessels

Manufacturing

Vessel Preparation

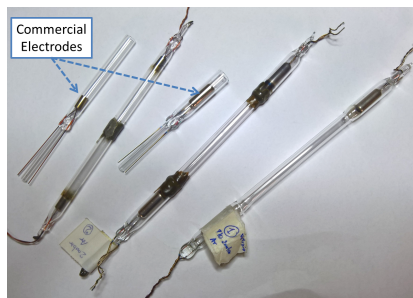
Commercial electrodes sealed with a tube of the desired dimensions



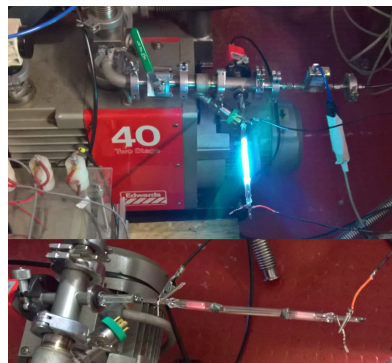
Manufacturing

Vessel Preparation

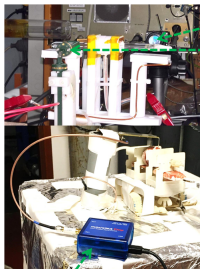
Commercial electrodes sealed with a tube of the desired dimensions



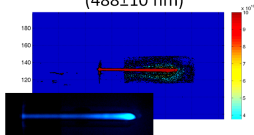
Aging process



Diagnostic

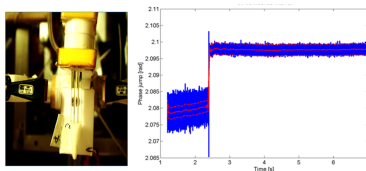


Basler Camera with BP filters
(488 ± 10 nm)

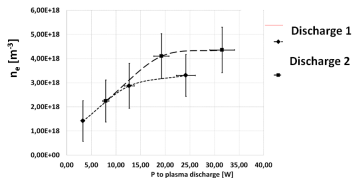


Filtered image of a plasma discharge, and plasma density map.

MW Interferometer

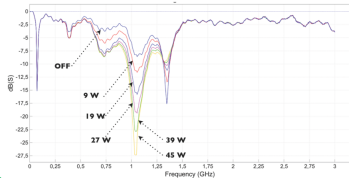


Plasma density value is correlated to the phase jump.



Plasma density against the net power to plasma.

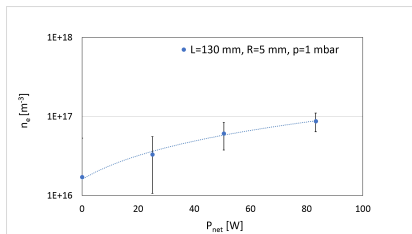
VNA



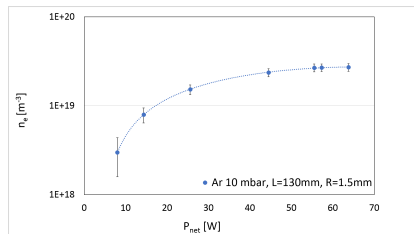
Magnitude of the reflection coefficient of the plasma dipole without plasma ("OFF"), and at different net power to plasma

Source Characterization

RF Discharges



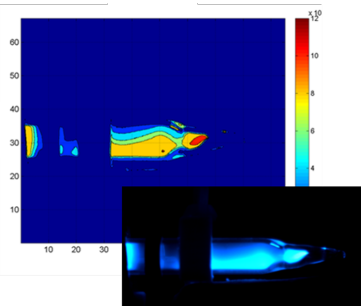
Argon, $p_n = 1$ mbar,
 $\Phi = 10$ mm, $L = 130$ mm.



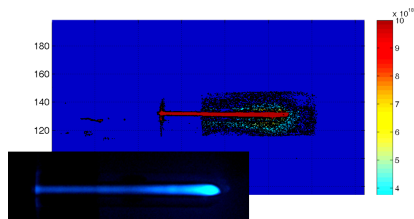
Argon, $p_n = 10$ mbar,
 $\Phi = 3$ mm, $L = 130$ mm.

Source Characterization

RF Discharges



Argon, $p_n = 1$ mbar,
 $\Phi = 10$ mm, $L = 130$ mm.



Argon, $p_n = 10$ mbar,
 $\Phi = 3$ mm, $L = 130$ mm.

Source Characterization

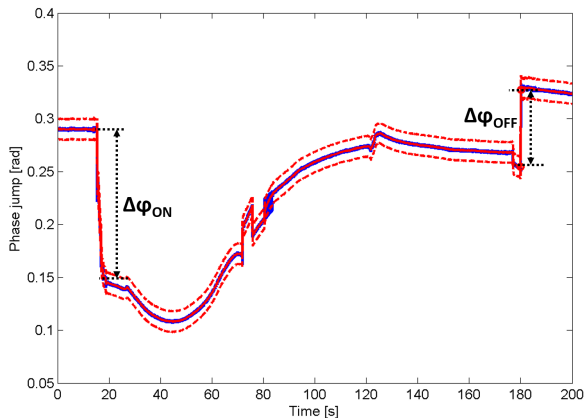
HF Discharges

We explored different gas pressures, and mixture

| Gas | p_n [mbar] | n_0 [m^{-3}] |
|---------|--------------|---|
| Ar | 1 | $3.70 \cdot 10^{18} \pm 1.84 \cdot 10^{17}$ |
| Ar - Ne | 2 | $3.84 \cdot 10^{18} \pm 8.57 \cdot 10^{16}$ |
| Ar | 2 | $4.40 \cdot 10^{18} \pm 5.09 \cdot 10^{17}$ |
| Ar - Hg | 2 | $3.18 \cdot 10^{18} \pm 5.88 \cdot 10^{16}$ |
| Ar - Hg | 1 | $2.59 \cdot 10^{18} \pm 1.50 \cdot 10^{17}$ |

Source Characterization

HF Discharges

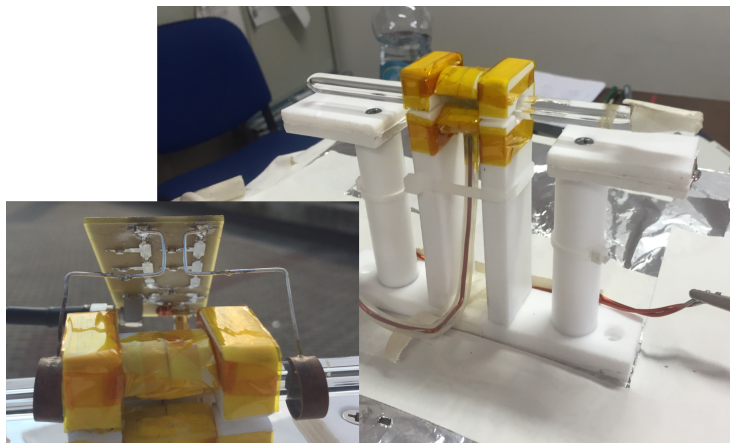


$$n_{ON} = 5.08 \cdot 10^{18} \pm 3.38 \cdot 10^{17} \text{ m}^{-3}$$

$$n_{OFF} = 2.83 \cdot 10^{18} \pm 4.11 \cdot 10^{17} \text{ m}^{-3}$$

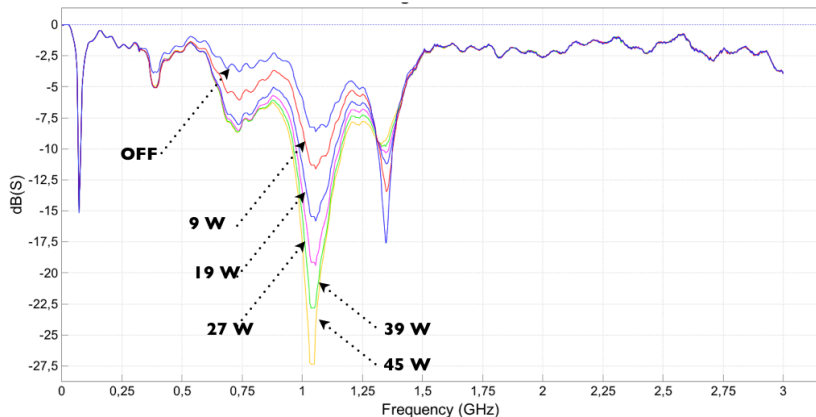
Antenna Characterization - Reflection Coefficient

Argon, $p_n = 10$ mbar, $\Phi = 3$ mm, $L = 130$ mm.



Antenna Characterization - Reflection Coefficient

Argon, $p_n = 10$ mbar, $\Phi = 3$ mm, $L = 130$ mm.

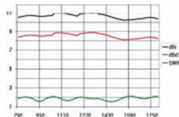
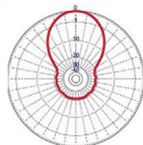
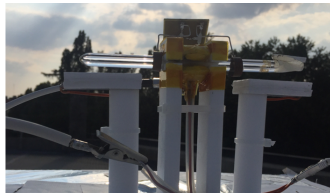
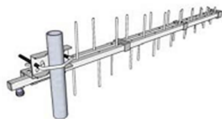


Antenna Characterization - Gain Pattern

Antenna testing with a well-known Log-Hallo Antenna as transmitter.

F53.027

LOG HALLO 790+1300 N

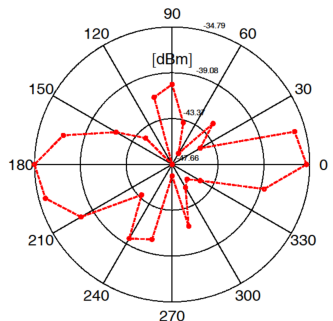


Friis Transmission Equation:

$$G_r = P_r - P_t - G_t - 10 \log_{10} \left(\frac{\lambda}{4\pi R} \right)^2$$

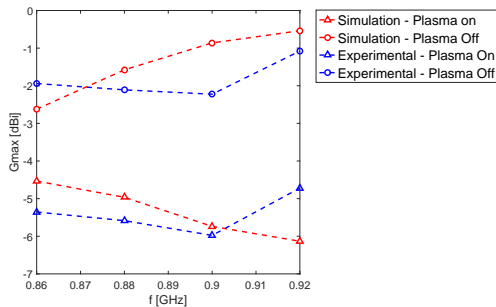
Antenna Characterization

P_r on the E-plane



$$G_{max} = -6 \text{ dBi}$$

G_{max} on the E-plane



Conclusions

- Development of a tool that couples the EM solution with the plasma transport, useful to study both GPAs, and Plasma Thrusters.
- Physical assessment on wave propagation in a plasma column.
- Physical assessment on the radiation properties of a plasma dipole.
- Design of 2 plasma sources to be exploited in a GPA.
- Preliminary assessment on the antenna performance of a GPA.

Publications

- Trezzolani, F., Magarotto, M., Manente, M., Moretto, D., Bosi, F.J., Gallina, G., De Carlo, P., Melazzi, D., Pavarin, D., Pessana, M., *Development of a counterbalanced pendulum thrust stand for electric propulsion*, (2017) 4th IEEE International Workshop on Metrology for AeroSpace, MetroAeroSpace 2017 - Proceedings, art. no. 7999554, pp. 152-157.
- Melazzi, D., De Carlo, P., Trezzolani, F., Lancellotti, V., Manente, M., Pavarin, D., Rigobello, F., Capobianco, A.-D., *First experimental characterization of a gaseous plasma antenna in the UHF band*, (2017) 2017 11th European Conference on Antennas and Propagation, EUCAP 2017, art. no. 7928419, pp. 3213-3217.
- Melazzi, D., De Carlo, P., Lancellotti, V., Trezzolani, F., Manente, M., Pavarin, D., *Radiation properties of a Gaseous Plasma dipole*, (2016) 2016 10th European Conference on Antennas and Propagation, EuCAP 2016, art. no. 7481458.
- Melazzi, D., De Carlo, P., Manente, M., Pavarin, D., *Gaseous plasma antenna array for GPS: Overview and development status*, (2015) Proceedings of the 2015 International Conference on Electromagnetics in Advanced Applications, ICEAA 2015, art. no. 7297264, pp. 997-1000.
- Melazzi, D., De Carlo, P., Manente, M., Lancellotti, V., Pavarin, D., *Numerical results on the performance of gaseous plasma antennas*, (2015) Proceedings of the 2015 International Conference on Electromagnetics in Advanced Applications, ICEAA 2015, art. no. 7297180, pp. 569-572.
- Trezzolani, F., Bosi, F., Melazzi, D., De Carlo, P., Selmo, A., Manente, M., Ferraris, S., Pessana, M., Pavarin, D., *Development of a kW-level plasma thruster in project SAPERE-STRONG*, (2015) Proceedings of the International Astronautical Congress, IAC, 10, pp. 8106-8113.

THANKS FOR YOUR ATTENTION

